

Article

Double-Layer Capacitances Caused by Ion–Solvent Interaction in the Form of Langmuir-Typed Concentration Dependence

Koichi Jeremiah Aoki ¹, Ridong He ^{2,3} and Jingyuan Chen ^{2,*} ¹ Electrochemistry Museum, Fukui 910-0804, Japan; kaoki@u-fukui.ac.jp² Department of Applied Physics, University of Fukui, 3-9-1 Bunkyo, Fukui 910-0017, Japan; HE729308012@163.com³ College of Chemical Engineering, Inner Mongolia University of Technology, Hohhot 010051, China

* Correspondence: jchen@u-fukui.ac.jp; Tel.: +81-9082625425

Abstract: Variations of the double layer capacitances (DLCs) at a platinum electrode with concentrations and kinds of salts in aqueous solutions were examined in the context of facilitating orientation of solvent dipoles. With an increase in ionic concentrations, the DLCs increased by ca. a half and then kept constant at concentrations over 1 mol dm⁻³. This increase was classically explained in terms of the Gouy–Chapman (GC) equation combined with the Stern model. Unfortunately, measured DLCs were neither satisfied with the Stern model nor the GC theory. Our model suggests that salts destroy hydrogen bonds at the electrode–solution interface to orient water dipoles toward the external electric field. A degree of the orientation depends on the interaction energy between the salt ion and a water dipole. The statistical mechanic calculation allowed us to derive an equation for the DLC as a function of salt concentration and the interaction energy. The equation took the Langmuir-type in the relation with the concentration. The interaction energy was obtained for eight kinds of salts. The energy showed a linear relation with the interaction energy of ion–solvent for viscosity, called the *B*-coefficient.

Keywords: variation of capacitance with salt concentrations; destroyed hydrogen bonds by salts; relation of capacitance with viscosity; grand canonical ensemble



Citation: Aoki, K.J.; He, R.; Chen, J. Double-Layer Capacitances Caused by Ion–Solvent Interaction in the Form of Langmuir-Typed Concentration Dependence. *Electrochem* **2021**, *2*, 631–642. <https://doi.org/10.3390/electrochem2040039>

Academic Editor: Masato Sone

Received: 1 October 2021

Accepted: 17 November 2021

Published: 18 November 2021

Publisher's Note: MDPI stays neutral with regard to jurisdictional claims in published maps and institutional affiliations.



Copyright: © 2021 by the authors. Licensee MDPI, Basel, Switzerland. This article is an open access article distributed under the terms and conditions of the Creative Commons Attribution (CC BY) license (<https://creativecommons.org/licenses/by/4.0/>).

1. Introduction

Double-layer capacitances (DLCs) used for an electric energy storage [1,2] have been developed to enhance the output energy, the power, and the cycle stability [3,4]. The development has been directed to:

- increasing geometrical, active area of electrodes by use of porous electrodes or powder electrodes [5];
- decreasing solution resistance by selecting combinations of solvents with salts [6];
- expanding electrochemically inactive voltage domains [7,8], such as by use of ionic liquids.

Especially, item (b) belongs to a simply chemical handling in examining various kinds of ions and their concentrations in appropriate solvents. It only deforms charge–discharge curves by the ohmic drop [9], but does not essentially improve DLCs because a DLC is caused mostly by orientation of solvent dipoles for relaxing the electric field in the Helmholtz layer [10,11].

Ionic effects of the DLCs have sometimes been thought to be expressed by the Gouy–Chapman (GC) theory, which exhibits V-shaped capacitance vs. voltage curves. However, no V-shape has been found even in 0.05-mM salts [12]. DLC values have not been obeyed by the dependence of the square-root of concentrations predicted from the GC theory [13]. The drawback of the GC theory is the extra condensation of ions beyond the finite size of ions [14]. However, it fails to explain the indistinctively small contribution of ions to

the DLC in comparison with the Helmholtz capacitance [15]. The weak salt dependence obtained in the fundamental studies is inconsistent with industrial efforts of enhancing ionic conductance [4,16–19]. The challenge of examining concentration dependence [20–26] cannot be covered with thermodynamic bases.

The DLCs also vary with time scales of measurements. A well-known time dependence is frequency dispersion [27], which has been empirically recognized as the concept of the constant phase element (CPE) [28–31] or explained in terms of the power law of the frequency [10,11,32,33]. The salt effects should be taken into account together with the frequency dispersion. If the frequency-dispersed DLC values were extrapolated to zero frequency or under a steady state, they would be diverged owing to the power law. Therefore, applications of the Poisson–Boltzmann distribution under the steady state are not, in principle, satisfied with the experimental conditions. In contrast, a short time extreme has been made in molecular dynamic studies [34–38] in which the time scales are as short as pico seconds. The time difference in nine powers in magnitude from the experimental conditions yields ten times larger than the experimental values of DLCs by applying the frequency dispersion. Therefore, it is necessary to take into account both the frequency dispersion and the salt effects.

Ions alter DLC values only by a certain degree. This secondary effect motivates us to consider the interaction between ions and solvent dipoles, an example of which is a relationship between ions and hydrogen bond structure, addressed by Frank [39] and Samoilov [40]. The relation has been represented experimentally as Jones–Dole viscosity *B*-coefficients [41,42], hydration activation energies by ions [43], ion solvation thermodynamics [44,45], and Setschenow coefficients (salting out) [46,47]. These relations are predicted to express the ionic effects on the DLCs. These secondary effects should be discriminated against ion–ion interactions, such as in the Debye theory and the GC theory.

We discuss in this work the ionic effect on the DLCs in the light of the interaction of hydrogen bonds with ions in the comparison with the viscosity of *B*-coefficients. The *B*-coefficients are empirical values determined from a slope of the viscosity against ionic concentrations. In contrast, there is a theoretical prospect that the DLC can be expressed as the interaction energy and ionic concentration through statistical mechanics. We derive here an equation for the ionic contribution to the DLC, which will have a Langmuir type. We measure frequency-dispersed DLCs in various concentrations of eight kinds of mono-valent salts at a platinum wire electrode in order to clarify the ionic contribution.

2. Materials and Methods

A platinum wire, with a diameter of 0.5 mm, was used for a working electrode. It was put into mixed acid ($\text{H}_3\text{PO}_4 + \text{HNO}_3 + \text{CH}_3\text{COOH}$, vol. 2:1:1) to remove oxides on the surface [48]. It was immersed into the aqueous test solution by a given length, ca. 8 mm, which was determined accurately with an optical microscope. Since the wire was not sealed with any insulating material, it can avoid floating capacitive current at a gap between the electrode and the insulator. The counter electrode was a platinum wire with the area 100 times larger than that of the working electrode, and the reference electrode was Ag–AgCl in saturated KCl solution. The test solution was deaerated for 20 min before the voltage application. Aqueous solutions of LiCl, NaCl, KCl, HCl, CsNO_3 , KNO_3 , NaNO_3 , and NaOH were prepared with reagents at the analytical grade and the deionized water prepared by CPW-100 (Advantec, Tokyo).

The potentiostat was Compactstat (Ivium, The Netherlands) for ac impedance measurements and cyclic voltammetry. Conditions of ac impedance were the frequency range from 0.2 Hz to 5000 Hz with the amplitude of 10 mV. All measurements were made at temperature of 25 ± 1 °C. Voltammetric reproducibility was examined at each experimental run. Reproducibility of our voltage time curves was examined at three runs to be within 5% errors.

3. Theory

Our basic concept of an effect of ions on DLCs is to consider competition between hydration of ions and orientation of water dipoles by the external field. For example, we compare degrees of hydration on Li^+ and Na^+ in the vicinity of an electrode for a common anion. Li^+ is more strongly hydrated than Na^+ to exhibit a hydration radius of Li^+ larger than of Na^+ . It makes the dipoles oriented more radially than Na^+ . As a result, the dipoles located between the Li^+ and the electrode may relax more strongly in the external field than those for Na^+ , yielding higher DLCs in Li^+ solution. A thermodynamic measure of hydration is the interaction energy between ions and water molecules. We incorporate this energy to the ionic effect on DLCs.

In order to orient dipoles of water molecules on an electrode by the external field for impedance measurements, the dipoles have to destroy hydrogen bonds with which they have formed their own surface structure. Since the interaction energy of the water dipoles is at least ten times larger than the field-oriented energy [33], only a small part of water molecules can be oriented with the field, overcoming the structuralization by hydrogen bonds. This is why values of the DLCs have been observed to be much smaller than those predicted from a parallel plate capacitive model in the Helmholtz layer, as represented by the saturated permittivity [11,49–51]. In other words, the dipoles to be oriented are released from the restriction of the hydrogen bonds by thermal fluctuation.

The ionic contribution of the DLC is proportional to the number of oriented dipoles which are suppressed by ions against the hydrogen bond. We let the latent number of dipoles oriented by the electric field be M at the solution–water interface in N ions on the interface. We define the energy with which an ion can orient a water dipole as $-u$, and let the chemical potential of the ion be μ . Then, the energy of orienting the N dipoles is given by $N\{-\mu + (-u)\}$. Large values of u promote orientation and, hence, increase the DLCs. This energy represents the probability of the number of the oriented dipoles through the Boltzmann distribution, $\exp[\beta(\mu + u)N]$, where $\beta = 1/k_{\text{B}}T$ with the Boltzmann constant k_{B} at the temperature T . Since N ions are selected from M dipoles randomly, there are $M!/N!(M - N)!$ combinations so that the probability is given by $P(N) = \{M!/N!(M - N)!\} \exp[\beta(\mu + u)N]$. Since each probability takes part in the orientation, the observed probability is a sum for N ranging from 0 to M :

$$\Xi = \sum_{N=0}^M P(N) = (1 + \exp[\beta(\mu + u)])^M \quad (1)$$

This is the partition function for the grand canonical ensemble. We assume that there is no adsorption of ions or that the ionic concentration at the interface keeps the value in the bulk, and that the ion with concentration c behaves as an ideal solution such that the chemical potential can be expressed by $\mu = \mu^\circ + k_{\text{B}}T \ln(c/c^\circ)$. Eliminate μ from Equation (1) yields

$$\Xi = \{1 + (c/c^\circ) \exp[\beta(\mu^\circ + u)]\}^M \quad (2)$$

The ionic contribution of the DLC is proportional to the averaged N :

$$\langle N \rangle = \sum_{N=0}^M NP(N) / \Xi = k_{\text{B}}T (\partial \Xi / \partial u) / \Xi$$

Inserting Equation (2) into the above and carrying out the differentiation yields

$$\langle N \rangle / M = 1 / \{1 + (c^\circ/c) \exp[-\beta(\mu^\circ + u)]\} \quad (3)$$

This is equivalent to the normalized DLC for the ionic contribution. Equation (3) is the same form as the Langmuir adsorption isotherm.

Variations of $\langle N \rangle / M$ with c/c° are shown in Figure 1 for some values of $\beta(\mu^\circ + u)$. A problem is a technique of extracting only the ionic contribution from the observed DLC. Equation (3) indicates that plots of the inverse of the ionic contribution against $1/c$ should take a line with the intercept 1.

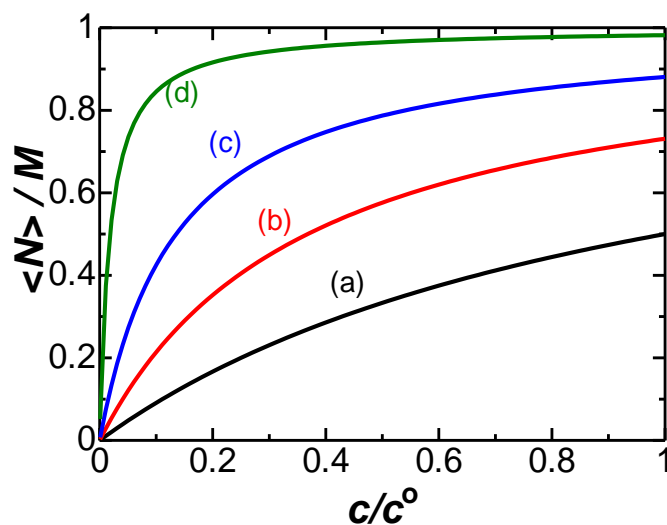


Figure 1. Variations of $\langle N \rangle / M$ with c/c^0 calculated from Equation (3) for $(\mu^0 + u)/k_B T =$ (a) 0, (b) 1, (c) 2, and (d) 4.

4. Results and Discussion

Nyquist plots of the real impedance, Z_1 , vs. the imaginary one, Z_2 , at the Pt wire electrode in 0.5 M of LiCl, HCl, and KCl solutions fell on each line with slope ranging from 5 to 8, as shown in Figure 2. The deviation of the slopes from the infinite (a vertical line) stands for the frequency dispersion of the DLC. Letting the application of ac voltage be $V = V_{ac}e^{i\omega t}$ for the angular velocity ω and the imaginary unit i , the observed ac current density responding to the voltage is expressed as the time derivative of the charge, CV , i.e., [15]

$$j = d(CV)/dt = V\{-2\pi f^2 (dC/df) + i\omega C\} \quad (4)$$

where f is the frequency ($= \omega/2\pi$). This can be represented as the resistance-subtracted admittance,

$$j/V \equiv Y = Y_1 + iY_2 = -2\pi f^2(dC/df) + i\omega C \quad (5)$$

where

$$Y_1 = (Z_1 - R_s)/\{(Z_1 - R_s)^2 + Z_2^2\} \quad (6)$$

$$Y_2 = -Z_2/\{(Z_1 - R_s)^2 + Z_2^2\} \quad (7)$$

Here, R_s is the solution resistance determined by extrapolating the Nyquist plot to $Z_2 = 0$. Equations (6) and (7) state that $Y_2/Y_1 = -Z_2/(Z_1 - R_s)$, of which values are constant from the slopes in Figure 2. We set the constant slope to be $1/\lambda$. Replacing Y_1 and Y_2 by $-2\pi f^2(dC/df)$ and ωC , respectively, by use of Equations (6) and (7), we obtain the differential equation, $-2\pi f^2(dC/df)/\omega C = \lambda$ or $-f(dC/df)/C = \lambda$. A solution is

$$C = C_1 f^{-\lambda} \quad (8)$$

where C_1 is the capacitance value at $f = 1$ Hz. Elimination of C in Equation (6) by use of Equation (8) yields the expression for the admittance

$$Y = (\lambda + i) \omega C = 2\pi(\lambda + i)C_1 f^{-\lambda+1} \quad (9)$$

or

$$\log Y_2 = \log(2\pi C_1) + (1 - \lambda)\log f \quad (10)$$

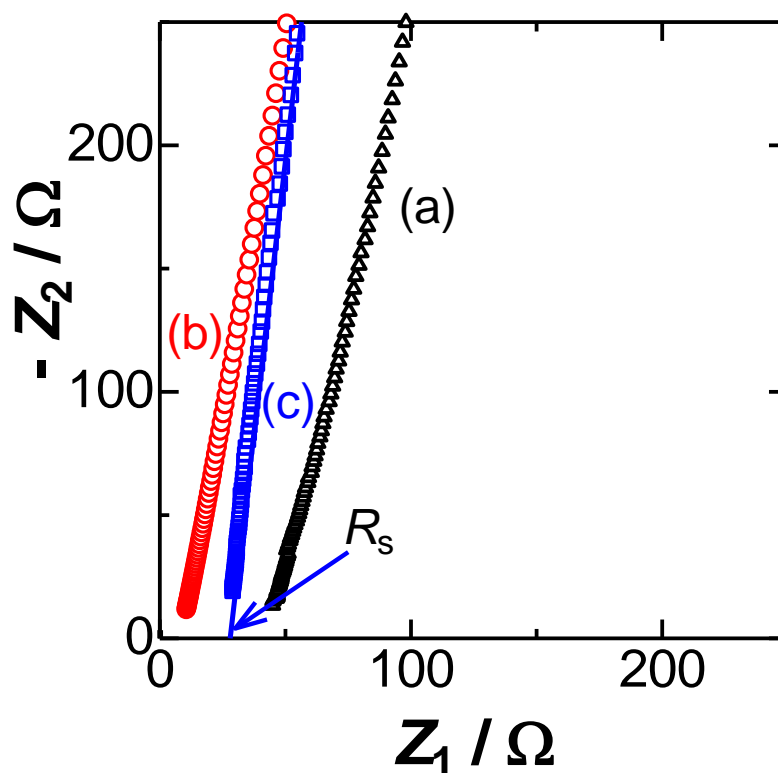


Figure 2. Nyquist plots in the aqueous solutions of 0.5 M (a) LiCl, (b) HCl, and (c) KCl.

All the plots of $\log Y_2$ against $\log f$ showed lines with correlation coefficients close to 0.9999 for $1 \text{ Hz} < f < 5000 \text{ Hz}$. Values of λ obtained from the slopes ($1 - \lambda$) ranged from 0.09 to 0.11. Therefore, Equation (9) holds commonly for all the salts and the concentration ranges used here. Non-zero values of λ suggest the CPE behavior. Plots of $\log Y_1$ vs. $\log f$ showed the behavior similar to those of $\log Y_2$. They included noises more than $\log Y_2$ because of $Y_1 \approx Y_2/10$.

We evaluated C_1 from the intercepts of the lines of the plots in Equation (10) at several concentration of salts, c , and plotted C_1 against c in Figure 3 for some salts. Values of C_1 at low concentrations increased linearly with an increase in c , and approached each constant value. The ratio of the increasing amount to C_1 was at most 1.5, depending on the kind of salts. A line extrapolated to $c = 0$ means an imaginary value of C_1 , which might be determined for $c = 0$ or in pure water. Therefore, the extrapolated values should be independent of the kinds of salts. Unfortunately, $(C_1)_{c=0}$ varied actually with a set of experimental runs. Iterative runs showed that the variation of $(C_1)_{c=0}$ was not caused by salts but was by history of the Pt electrode. A long-term use of the electrode increased $(C_1)_{c=0}$ probably because of an increase in the surface roughness by the iteratively chemical treatment with the mixed acid. In order to avoid the aging effect, we normalized C_1 at any value of c with $(C_1)_{c=0}$ at a given salt in the following discussion of the salt effects.

The GC theory predicts the proportionality of the DLCs to $c^{1/2}$, which inspired us to make C_1 vs. $c^{1/2}$ plots in the inset of Figure 3. The linear relation is found for $c < 0.2 \text{ M}$ although the GC theory is not only valid for $c < 0.05 \text{ mM}$ [12,52]. Consequently, our data are not satisfied with the GC theory. The $c^{1/2}$ dependence is caused by the Poisson–Boltzmann distribution, which is based on the electrostatic interaction of ion–field and ion–ion. The invalidity of the $c^{1/2}$ dependence implies that the ionic effect on the DLCs does not result from the electrostatic interaction.

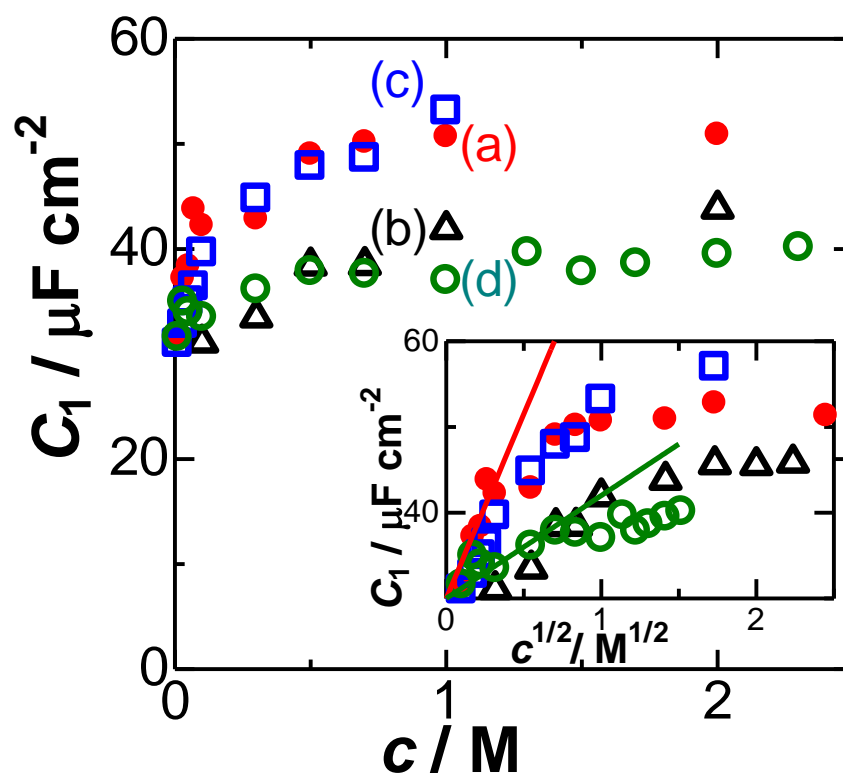


Figure 3. Variations of the capacitances at $f = 1$ Hz with concentrations, c , of (a) NaOH, (b) LiCl, (c) KCl, and (d) KNO₃, where values of C_1 is normalized to the averaged value, $30 \mu\text{F cm}^{-2}$. The inset is plots of C_1 against $c^{1/2}$ of the type of the GC theory.

If the DLCs obey the Stern model, i.e., a series combination of the Helmholtz capacitance, C_{Hm} , with the ionic capacitance, C_{ion} , by the GC theory, the observed DLC values should have a linear relation of $1/C_1$ with $c^{-1/2}$ (in Figure 4) through $1/C_1 = 1/C_{\text{Hm}} + 1/C_{\text{ion}}$, $= 1/C_{\text{Hm}} + kc^{-1/2}$, where C_{ion} is proportional to $c^{1/2}$ by the GC theory. The variations in Figure 4 have no linearity, and, hence, the Stern model is not suitable for the concentration variations of the DLCs. The concentration dependence in the previous report [53] has suggested a parallel combination of C_{Hm} and C_{ion} . This model is based on the following concept: Dipoles of solvent molecules are oriented both with and without aid of ionic interaction by the external electric field. We let the DLCs generated by the former and the latter dipoles be $(C_{\text{Hm}})_{c \neq 0}$ and $(C_{\text{Hm}})_{c = 0}$, respectively. Since the equivalent circuit of the two DLCs is a parallel combination, the observed DLC is given by the simple sum of the two

$$C_1 = (C_1)_{c=0} + (C_1)_{c \neq 0} \quad (11)$$

where $(C_1)_{c=0}$ corresponds to the averaged value of $30 \mu\text{F cm}^{-2}$ in Figure 3. In contrast, $(C_1)_{c \neq 0}$ corresponds to the increasing parts in Figure 3.

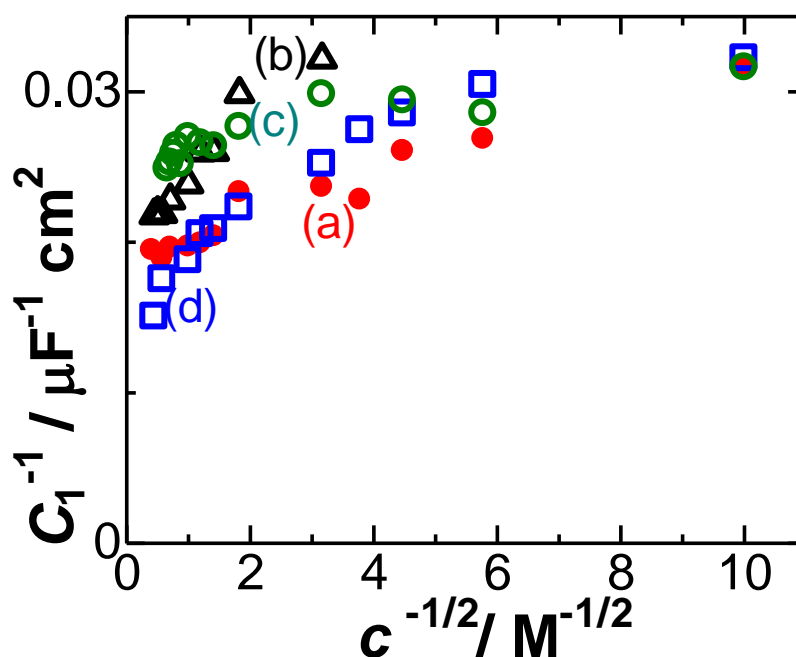


Figure 4. Stern-type plots of $1/C_1$ vs. $c^{-1/2}$ for the ions in Figure 3.

Our concern is the ionic contribution, $(C_1)_{c \neq 0}$. In order to apply Equation (3) to our experimental results, we normalized $(C_1)_{c \neq 0}$ with the difference between $(C_1)_{c = \text{high}}$ and $(C_1)_{c = 0}$ to denote

$$y = [(C_1)_{c \neq 0} - (C_1)_{c = 0}] / [(C_1)_{c = \text{high}} - (C_1)_{c = 0}] \quad (12)$$

Then, the inverse of Equation (3) can be rewritten as

$$1/y = 1 + K/c$$

where

$$K = c^0 \exp[-\beta(\mu^0 + u)] \quad (13)$$

Figure 5 shows dependence of the inverse of the normalized DLC through Equation (12) on $1/c$ for four salts. The plots fell on each line, passing through the unity intercept. Therefore, Equation (3) should hold for a given value of u . Equation (3') states that slopes of the lines in Figure 5 represent K . Equation (3) at low concentrations can be approximated as

$$C_1 / (C_1)_{c = 0} \approx 1 + Hc \quad (14)$$

where

$$H = \{(C_1)_{c = \text{high}} / (C_1)_{c = 0} - 1\} / K \quad (15)$$

Equation (14) has a form similar to the viscosity B -coefficient [41,42], $\eta / \eta_0 = 1 + Bc$, where η and η_0 are viscosities, respectively, for any concentration and $c = 0$. Figure 3 has demonstrated the linear relation of C_1 with c at low concentrations. Therefore, the term H can be regarded as equivalence to the B -coefficient. It is plotted in Figure 6 against the B -coefficients for eight kinds of salts. The enhancement of H with an increase in B supports that the ionic variations of the DLCs are caused by the interaction between ions and solvents. A difference of H from the B coefficients lies in the fact that signs of H were always positive while B can take negative values. In other words, ionic effects always enhance the DLCs whereas they increase or decrease viscosity depending on species.

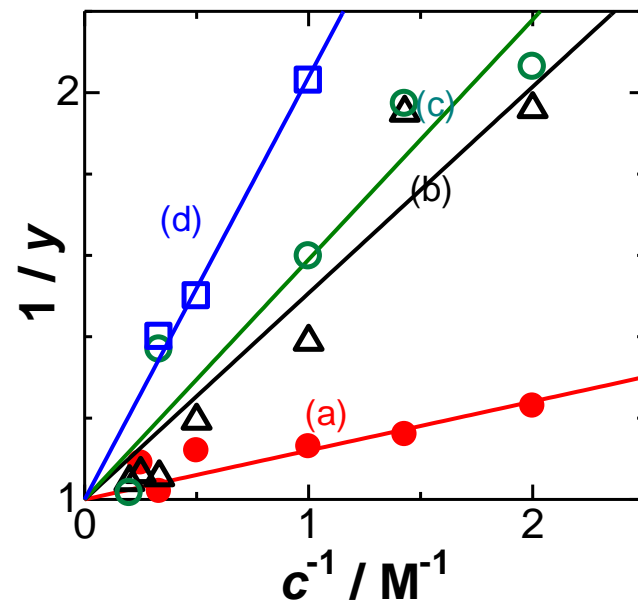


Figure 5. Dependence of the inverse of the normalized DLCs, y , on the inverse of concentrations of the salts specified in Figure 3.

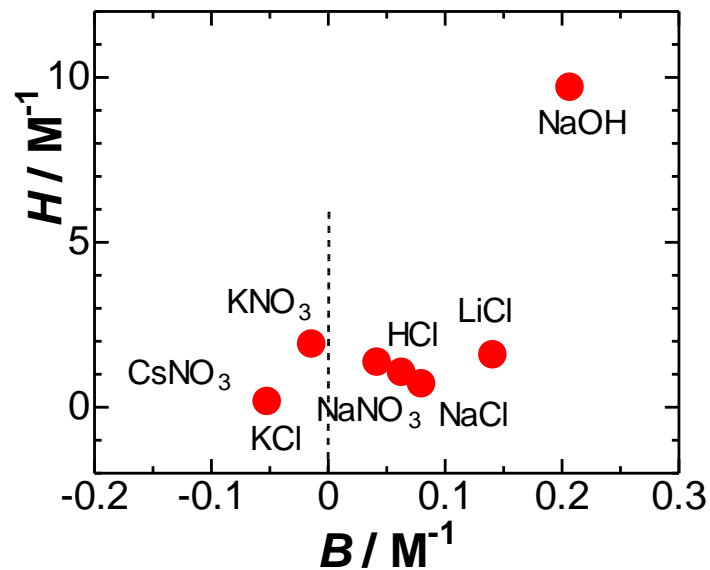


Figure 6. Dependence of the coefficient, H , in Equation (14) on the viscosity B -coefficient.

Equation (13) shows that $-\log K$ includes the interaction energy u , which may be related with the B coefficients. Figure 7 shows dependence of $u/k_B T$, being a part of $-\log K$, on the B coefficients. A linear relation indicates that the B coefficient should represent the ionic interaction energy with solvents rather than intensity variables such as viscosity or DLCs. The linear relation seems to be in abnormal behavior in that the ionic interaction energy has the linear relation with concentrations rather than logarithmic ones. This is due to the complicatedly dynamic mechanisms of Jones-Dole B -coefficients rather than a simple difference in free energy of interactions.

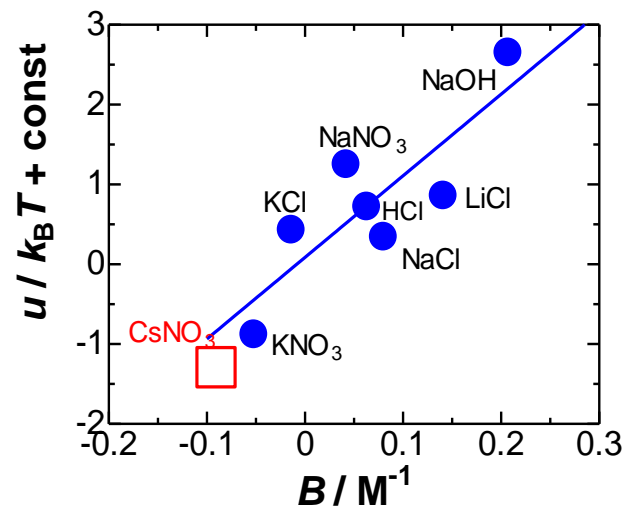


Figure 7. Dependence of $u/k_B T$ obtained in Figure 5 on the viscosity B -coefficients, where no value of $u/k_B T$ for CsNO_3 was determined explicitly.

The ionic interaction energy, u , releases water molecules from hydrogen bonds to orient the dipoles toward the external field. It seems to be close to the free energy of hydration of ions in water. A number of the data on the hydration have been compiled [44], which can be used for comparison with our evaluated energy. Available data are the Gibbs free energy of interaction of ions hydrated with water in infinitely diluted solution, $\Delta_{\text{hyd}}G$ [44]. The dimensionless energies are plotted in Figure 8, exhibiting a positive correlation except for HCl. The correlation indicates that the ionic enhancement of the DLCs should be brought about by hydration of ions, which corresponds to the destruction of hydrogen bonds by ions to facilitate orientation by the field. The slope of the linearity is 0.03. This extremely small value suggests only 3% contribution of the hydration to the DLCs, not only because of the one-directional orientation by the external electric field from multi-directional orientations by ions but also because of difference in the number of oriented dipoles.

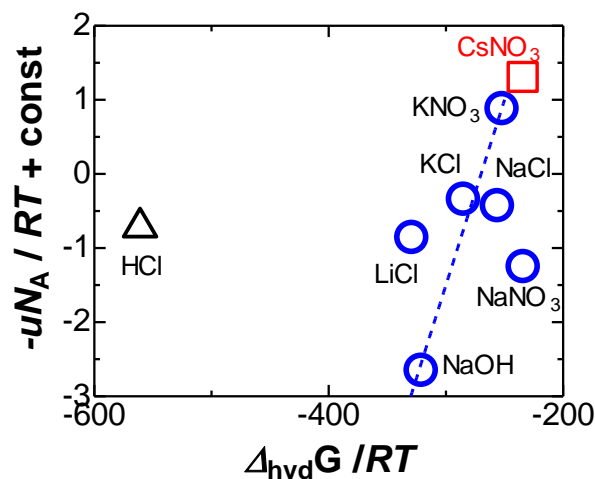


Figure 8. Variation of the interaction energy of the DLCs with the Gibbs free energy of the hydration.

5. Conclusions

The experimentally conclusive results are that:

- (i) values of DLCs increase with ionic concentrations and reach saturated values at most 1.5 times as large as the ion-free value;
- (ii) the values are not at all proportional to $c^{1/2}$ by the GC theory;

- (iii) the Stern model is not valid in the context of the concentration dependence;
- (iv) ionic effects are caused by ion–solvent interaction rather than ion–ion interaction;
- (v) variation of C_1 with c depends on ionic properties.

In particular, item (ii) controverts the participation in ion–ion interaction which has been classically employed through the Poisson–Boltzmann equation or the GC theory.

The ionic contribution of the DLC can be formulated through the following model. An ion relaxes a hydrogen-bonded water molecule in the Helmholtz layer by the amount of the ion–water interaction energy so that the water dipole may be oriented with the external electric field. The average number of the oriented dipoles provides the ionic contribution of the DLC. It can be derived through the grand canonical statistical mechanics, yielding the dependence of the capacitance on the concentrations with a Langmuir type. The ionic contribution can be extracted through the parallel combination model rather than the Stern model, according to the previous work.

DLC values for eight salts at various concentrations allows us to determine the ion–water interaction energy, which is specific to each ion. The energy has the strong correlation with the viscosity B -coefficients, which stands for the ion–solvent interaction. It also shows correlation with available hydration energy of ions.

Author Contributions: Conceptualization, K.J.A. and J.C.; methodology, R.H.; software, R.H.; validation, K.J.A., J.C. and R.H.; formal analysis, R.H.; investigation, R.H.; resources, J.C.; data curation, K.J.A. and J.C.; writing—original draft preparation, K.J.A.; writing—review and editing, K.J.A. and J.C.; visualization, R.H.; supervision, J.C.; project administration, K.J.A.; funding acquisition, J.C. All authors have read and agreed to the published version of the manuscript.

Funding: This research received no external funding.

Institutional Review Board Statement: Not applicable.

Informed Consent Statement: Not applicable.

Data Availability Statement: Not applicable.

Conflicts of Interest: The authors declare no conflict of interest.

References

1. Conway, B.E. *Electrochemical Supercapacitors: Scientific Fundamentals and Technological Applications*; Plenum Press: New York, NY, USA, 1999.
2. Lu, M.; Beguin, F.; Frackowiak, E. *Supercapacitors: Materials, Systems, and Applications*, 1st ed.; Wiley-VCH: Weinheim, Germany, 2013.
3. Kötz, R.; Carlen, M. Principles and applications of electrochemical capacitors. *Electrochim. Acta* **2000**, *45*, 2483–2498. [[CrossRef](#)]
4. Wang, G.; Zhang, L.; Zhang, J. A review of electrode materials for electrochemical supercapacitors. *Chem. Soc. Rev.* **2012**, *41*, 797–828. [[CrossRef](#)] [[PubMed](#)]
5. Ho, J.; Jow, E.; Boggs, S. Historical Introduction to Capacitor Technology. *IEEE Elect. Ins. Mag.* **2010**, *26*, 20–25. [[CrossRef](#)]
6. Namisnyk, A.M. A Survey of Electrochemical Supercapacitor Technology 2007. Available online: <https://www.semanticscholar.org/paper/A-SURVEY-OF-ELECTROCHEMICAL-SUPERCAPACITOR-Namisnyk-Zhu/d9018594f7d9a6cc36b7b0a11e8ea8fe55190a90> (accessed on 1 October 2021).
7. Evans, D.A. High Energy Density Electrolytic-Electrochemical Hybrid Capacitor. In *14th Capacitor & Resistor Technology Symposium*; Components Technology Institute Inc.: Jupiter, FL, USA, 22 March 1994.
8. Viswanathan, A.; Shetty, A.N. Enhancement of supercapacitance of reduced graphene oxide, copper oxide and polyaniline using the mixture of methane sulphonic acid and sulphuric acid as electrolyte. *Chem. Eng. Sci.* **2021**, *229*, 116020. [[CrossRef](#)]
9. He, R.; Aoki, K.J.; Chen, J. Electric Field-Dependence of Double Layer Capacitances by Current-Controlled Charge-Discharge Steps. *Electrochem* **2020**, *1*, 217–225. [[CrossRef](#)]
10. Hou, Y.; Aoki, K.J.; Chen, J.; Nishiumi, T. Solvent Variables Controlling Electric Double Layer Capacitance at Metal-Solution Interface. *J. Phys. Chem. C* **2014**, *118*, 10153–10158. [[CrossRef](#)]
11. Hou, Y.; Aoki, K.J.; Chen, J.; Nishiumi, T. Invariance of double layer capacitance to polarized potential in halide solutions. *Univ. J. Chem.* **2013**, *1*, 162–169. [[CrossRef](#)]
12. Zhao, X.; Aoki, K.J.; Chen, J.; Nishiumi, T. Examination of the Gouy–Chapman theory for double layer capacitance in deionized latex suspensions. *RSC Adv.* **2014**, *4*, 63171–63181. [[CrossRef](#)]
13. Khademi, M.; Barz, D.P.J. Structure of the Electrical Double Layer Revisited: Electrode Capacitance in Aqueous Solutions. *Langmuir* **2020**, *36*, 4250–4260. [[CrossRef](#)]

14. Bard, A.J.; Faulkner, L.R. *Electrochemical Methods: Fundamentals and Applications*; John Wiley & Sons, Inc.: New York, NY, USA, 2001; p. 551.
15. Aoki, K.J.; Chen, J. Effects of the dipolar double layer on elemental electrode processes at micro- and macro-interfaces. *Faraday Discuss.* **2018**, *210*, 219–234. [[CrossRef](#)] [[PubMed](#)]
16. Prehal, C.; Koczwara, C.; Amenitsch, H.; Presser, V.; Paris, O. Salt concentration and charging velocity determine ion charge storage mechanism in nanoporous supercapacitors. *Nat. Commun.* **2018**, *9*, 4145. [[CrossRef](#)]
17. Ramachandran, R.; Wang, F. *Electrochemical Capacitor Performance: Influence of Aqueous Electrolytes*; IntechOpen: London, UK, 2017.
18. Pohlmann, S.; Balducci, A. A new conducting salt for high voltage propylene carbonate-based electrochemical double layer capacitors. *Electrochim. Acta* **2013**, *110*, 221–227. [[CrossRef](#)]
19. Galek, P.; Frackowiak, E.; Fi, K. Interfacial aspects induced by saturated aqueous electrolytes in electrochemical capacitor applications. *Electrochim. Acta* **2020**, *20*, 135572. [[CrossRef](#)]
20. Li, J.; Pham, P.H.Q.; Zhou, W.; Pham, T.D.; Burke, P.J. Carbon-Nanotube–Electrolyte Interface: Quantum and Electric Double Layer Capacitance. *ACS Nano* **2018**, *12*, 9763–9774. [[CrossRef](#)] [[PubMed](#)]
21. Kortschot, R.J.; Philipse, A.P.; Ern , B.H. Debye Length Dependence of the Anomalous Dynamics of Ionic Double Layers in a Parallel Plate Capacitor. *J. Phys. Chem. C* **2014**, *118*, 11584–11592. [[CrossRef](#)]
22. Lust, E.; J nes, A.; Sammelseg, V.; Miidla, P. Influence of charge density and electrolyte concentration on the electrical double layer characteristics at rough cadmium electrodes. *Electrochim. Acta* **2000**, *46*, 185–191. [[CrossRef](#)]
23. Zhang, X.; Kuhnel, R.-S.; Passerini, S.; Balducci, A. Double-Salt Electrolytes for High Voltage Electrochemical Double-Layer Capacitors. *J. Sol. Chem.* **2015**, *44*, 528–537. [[CrossRef](#)]
24. Krummacher, J.; Balducci, A. Al(TFSI)₃ as a Conducting Salt for High-Voltage Electrochemical Double-Layer Capacitors. *Chem. Mater.* **2018**, *30*, 4857–4863. [[CrossRef](#)]
25. Uchida, S.; Masese, T. Electric Double-Layer Capacitors Based on Non-Aqueous Electrolytes: A Comparative Study of Potassium and Quaternary Ammonium Salts. *Batter. Supercaps* **2020**, *3*, 392–396. [[CrossRef](#)]
26. Zheng, J.P.; Jow, T.R. The Effect of Salt Concentration in Electrolytes on the Maximum Energy Storage for Double Layer Capacitors. *J. Electrochem. Soc.* **1997**, *144*, 2417–2420. [[CrossRef](#)]
27. Noel, R.L.; Hampson, A. The dispersion of double-layer capacitance with frequency I. Smooth solid electrodes. *Surf. Tech.* **1978**, *7*, 151–155.
28. Nyikos, L.; Pajkossy, T. Fractal dimension and fractional power frequency-dependent impedance of blocking electrodes. *Electrochim. Acta* **1985**, *30*, 1533–1540. [[CrossRef](#)]
29. Brug, G.J.; Van Den Eeden, A.L.G.; Sluyters-Rehbach, M.; Sluyters, J.H. The analysis of electrode impedances complicated by the presence of a constant phase element. *J. Electroanal. Chem.* **1984**, *176*, 275–295. [[CrossRef](#)]
30. Zoltowski, P. On the electrical capacitance of interfaces exhibiting constant phase element behavior. *J. Electroanal. Chem.* **1998**, *443*, 149–154. [[CrossRef](#)]
31. Lasia, A. Electrochemical Impedance Spectroscopy and its Applications. In *Modern Aspects of Electrochemistry*; Conway, B.E., Bockris, J.O.M., White, R.E., Eds.; Springer: Boston, MA, USA; Volume 32. [[CrossRef](#)]
32. Wang, H.; Aoki, K.J.; Chen, J.; Nishiumi, T.; Zeng, X.; Ma, X. Power law for frequency-dependence of double layer capacitance of graphene flakes. *J. Electroanal. Chem.* **2015**, *741*, 114–119. [[CrossRef](#)]
33. Aoki, K.J. Molecular interaction model for frequency-dependence of double layer capacitors. *Electrochim. Acta* **2016**, *188*, 545–550. [[CrossRef](#)]
34. Jiang, G.; Cheng, C.; Li, D.; Liu, J.Z. Molecular dynamics simulations of the electric double layer capacitance of graphene electrodes in mono-valent aqueous electrolytes. *Nano Res.* **2016**, *9*, 174–186. [[CrossRef](#)]
35. Welch, D.A.; Mehdi, B.L.; Hatchell, H.J.; Faller, R.; Evans, J.E.; Browning, N.D. Using molecular dynamics to quantify the electrical double layer and examine the potential for its direct observation in the in-situ TEM. *Adv. Struct. Chem. Imag.* **2015**, *1*, 1. [[CrossRef](#)]
36. Katakura, S.; Nishi, N.; Kobayashi, K.; Amano, K.; Sakka, T. An electric double layer structure and differential capacitance at the electrode interface of tributylmethylammonium bis(trifluoromethanesulfonyl)amide studied using a molecular dynamics simulation. *Phys. Chem. Chem. Phys.* **2020**, *22*, 5198–5210. [[CrossRef](#)]
37. Kong, X.; Lu, D.; Liu, Z.; Wu, J. Molecular dynamics for the charging behavior of nanostructured electric double layer capacitors containing room temperature ionic liquids. *Nano Res.* **2014**, *8*, 931–940. [[CrossRef](#)]
38. Burt, R.; Birkett, G.; Zhao, X.S. A review of molecular modelling of electric double layer capacitors. *Phys. Chem. Chem. Phys.* **2014**, *16*, 6519–6538. [[CrossRef](#)]
39. Frank, H.S.; Wen, W.-Y. Ion-Solvent Interaction. Structural Aspects of Ion-Solvent Interaction in Aqueous Solutions: A Suggested Picture of Water Structure. *Discuss. Faraday Soc.* **1957**, *44*, 133–140. [[CrossRef](#)]
40. Samoilov, O.Y. A new approach to the study of hydration of ions in aqueous solutions. *Discuss. Faraday Soc.* **1957**, *44*, 141–146. [[CrossRef](#)]
41. Feakins, D.; Lawrence, K.G. The relative viscosities of solutions of sodium and potassium chlorides and bromides in N-methylformamide at 25, 35, and 45°. *J. Chem. Soc. A* **1966**, 212–219. [[CrossRef](#)]
42. Jenkins, H.D.B.; Marcus, Y. Viscosity B-Coefficients of Ions in Solution. *Chem. Rev.* **1995**, *95*, 2695–2724. [[CrossRef](#)]
43. Talekar, S.V. Temperature dependence of activation energies for self-diffusion of water and of alkali ions in aqueous electrolyte solutions. A model for ion selective behavior of biological cells. *Int. J. Quantum Chem.* **1977**, *12*, 459–469. [[CrossRef](#)]

44. Marcus, Y. Thermodynamics of Solvation of Ions, Part 5. Gibbs Free Energy of Hydration at 298.15 K. *J. Chem. Soc. Faraday Trans.* **1991**, *87*, 2995–2999. [[CrossRef](#)]
45. Plambec, J.A. Solvation thermodynamics of ions: Free energies in water, ammonia, and fused LiCl-KCl eutectic. *Can. J. Chem.* **1969**, *47*, 1401–1410. [[CrossRef](#)]
46. Setschenow, J. Über die Konstitution der Salzlosungen auf Grund ihres Verhaltens zu Kohlensäure. *Z. Physik. Chem.* **1889**, *4*, 117–125. [[CrossRef](#)]
47. Ni, N.; Yalkowsky, S.H. Prediction of Setschenow constants. *Int. J. Pharm.* **2003**, *254*, 167–172. [[CrossRef](#)]
48. Aoki, K.J.; Chen, J.; Zeng, X.; Wang, Z. Decrease in double layer capacitance by Faradaic current. *RSC Adv.* **2017**, *7*, 22501–22509. [[CrossRef](#)]
49. Lust, E.; Jänes, A.; Arulepp, M. Influence of solvent nature on the electrochemical parameters of electrical double layer capacitors. *J. Electroanal. Chem.* **2004**, *562*, 33–42. [[CrossRef](#)]
50. Kim, I.-T.; Egashira, M.; Yoshimoto, N.; Morita, M. Effects of electrolytic composition on the electric double-layer capacitance at smooth-surface carbon electrodes in organic media. *Electrochim. Acta* **2010**, *55*, 6632–6638. [[CrossRef](#)]
51. Rampolla, R.; Miller, R.; Smyth, C. Microwave Absorption and Molecular Structure in Liquids. XXV. Measurements of Dielectric Constant and Loss at 3.1-mm Wavelength by an Interferometric Method. *J. Chem. Phys.* **1959**, *30*, 566. [[CrossRef](#)]
52. Aoki, K.J. Frequency-dependence of electric double layer capacitance without Faradaic reactions. *J. Electroanal. Chem.* **2016**, *779*, 117–125. [[CrossRef](#)]
53. Aoki, K.J.; He, R.; Chen, J. Parallel Combination of Inner Capacitance and Ionic Capacitance, Apparently Inconsistent with Stern's Model. *Electrochem* **2021**, *2*, 71–82. [[CrossRef](#)]